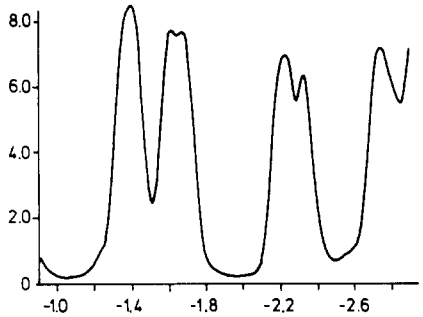

Figure 3. Differential-pulse polarogram of $[(Ru(bpy)_2)_2(bpt)]^{3+}$ (cation of **2**). The measurement has been carried out in acetonitrile with 0.1 M TBAP.

Table I. MLCT Bands and Reduction Potentials of the Mononuclear and Dinuclear Compounds with bpt

	abs band,[a] nm	redn potentials,[b] V
$[Bu(bpy)_2(bpt)]PF_6$ (**1**)	475 (1.13)	−1.47, −1.73, −2.27, −2.45, −2.55
$[(Ru(bpy)_2)_2(bpt)](PF_6)_3$ (**2**)	452 (2.26)	−1.40, −1.62, −1.67, −2.23, −2.33, −2.74

[a] Measured in ethanol; values in parentheses are extinction coefficients × 10^4. [b] Measured by using differential-pulse polarography in acetonitrile with 0.1 M tetraethylammonium perchlorate (TEAP). All values are versus SCE.

excitation to the π^* orbital of the dinucleating bpt ligand gives rise to a part of the MLCT band. If the bpt π^* orbital is populated, this can have important consequences for the nature of the emitting excited state.

In this note, the MLCT bands have been assigned by using rR spectroscopy and electrochemical measurements. With the use of these techniques, detailed information concerning the electronic structure of these compounds has been obtained.

Experimental Section

$[Ru(bpy)_2(bpt)]PF_6$ (**1**) and $[(Ru(bpy)_2)_2(bpt)](PF_6)_3$ (**2**) have been prepared as described previously.[2a] Purity has been checked by using NMR spectroscopy and elemental analysis.[2a] The rR spectra were recorded in CH_3CN solution by using a spinning cell and a Jobin Yvon HG2S Ramanor. The samples were excited by an SP Model 171 argon ion laser. Laser power was 50–100 mW and spectral slit width was 10 cm^{-1}. Excitation took place at 458, 488, and 514.5 nm. Electrochemical measurements have been carried out by using an EG&G Par C Model 303 with an EG&G 384B polarographic analyzer. The differential-pulse polarograms of the reduction potentials have been obtained at a scan rate of 4 mV/s with a pulse height of 20 mV.

Results and Discussion

The absorption spectra of $[Ru(bpy)_2(bpt)]^+$ (cation of **1**) and $[(Ru(bpy)_2)_2(bpt)]^{3+}$ (cation of **2**) are presented in Figure 2. Both compounds show MLCT bands around 450 nm, which is at an energy comparable to that of the Ru(II) → π^* transitions in $[Ru(bpy)_3]^{2+}$.[3a]

The differential-pulse polarogram of the dinuclear compound is shown in Figure 3. The reduction potentials and the energies of the MLCT bands are listed in Table I.

Because of the similarities of the reduction potentials of these compounds to those found for $[Ru(bpy)_3]^{2+}$, the peaks at about −1.40 and −1.72 V vs SCE have been assigned to the bpy-based reductions.[4]

The reduction of the bpt ligand is observed at a much more negative potential, and most probably the peaks at −2.23 and −2.33 V vs SCE can be explained by bpt-based reductions.

The rR spectra of the mononuclear compound (excitation at 458 and 514.5 nm, respectively) are presented in Figure 4. The vibrations of the bpy ligands are clearly observable at 1600, 1554, 1485, 1315, 1268, 1168, 1024, and 644 cm^{-1}. These assignments are based on a comparison with literature data of other $Ru(bpy)_x$ compounds.[3] Excitation at 488 nm yielded the same rR spectrum, and again, no bpt vibrations were resonance enhanced. Unfortunately, no rR spectra could be obtained with exciting laser lines having $\lambda > 514.5$ nm, because of disturbing luminescence. Similar results were obtained for the dinuclear compound, only vibrations of bpy being observed.

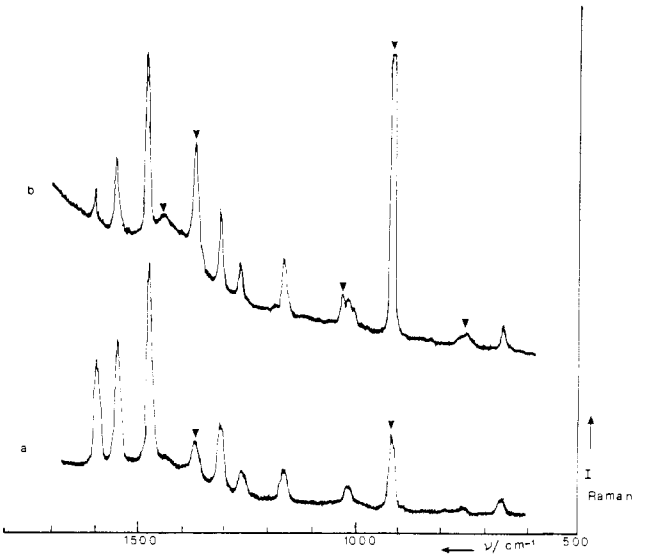

Figure 4. Resonance Raman spectrum of $[Ru(bpy)_2(bpt)]PF_6$ (**1**) in acetonitrile, obtained by excitation with λ = 458 nm (a) and λ = 514.5 nm (b). Bands indicated with a v are solvent bands.

These results clearly confirm the data obtained from the electrochemical measurements: the lowest energy MLCT band of compounds **1** and **2** can be explained by Ru → π^*(bpy) MLCT transitions. No transitions to π^*(bpt) orbitals are observed in this part of the absorption spectra.

Acknowledgment. We gratefully acknowledge the help of Ing. C. P. M. Montanus (Unilever Research Laboratorium, Vlaardingen, The Netherlands) with the electrochemical measurements. Furthermore, we wish to thank Johnson and Matthey Chemical Ltd. (Reading, U.K.) for their generous loan of $RuCl_3$.

Contribution from the Lehrstuhl für Anorganische Chemie I, Ruhr-Universität, D-4630 Bochum, FRG, and Anorganisch-Chemisches Institut der Universität, D-6900 Heidelberg, FRG

Preparation, Molecular Structure, and Magnetism of $[LFe(\mu\text{-}O)(\mu\text{-}CO_3)_2FeL]\cdot 4.25H_2O$ (L = 1,4,7-Trimethyl-1,4,7-triazacyclononane)

Stefan Drüeke,[1a] Karl Wieghardt,*[1a] Bernhard Nuber,[1b] and Johannes Weiss[1b]

Received November 2, 1988

The metalloprotein lactoferrin is known to reversibly bind two iron(III) ions concomitantly with two CO_3^{2-} (or HCO_3^-) groups.[2] A synergistic relationship between cation and anion binding has been established.[3] The determination of the crystal structure of human lactoferrin at 3.2-Å resolution[4] established that two oc-

(1) (a) Ruhr-Universität Bochum. (b) Universität Heidelberg.
(2) (a) Montreuil, J.; Tonnelat, J.; Mullet, S. *Biochim. Biophys. Acta* **1962**, *45*, 413. (b) Aisen, P.; Listowsky, I. *Annu. Rev. Biochem.* **1980**, *49*, 357. (c) Brock, J. H. *Top. Mol. Struct. Biol.* **1985**, *7*, 183.
(3) Cox, T. M.; Mazurier, J.; Spik, G.; Montreuil, J.; Peters, T. J. *Biochim. Biophys. Acta* **1979**, *588*, 120.
(4) (a) Anderson, B. F.; Baker, H. M.; Dodson, E. J.; Norris, G. E.; Rumball, S. V.; Waters, J. M.; Baker, E. N. *Proc. Natl. Acad. Sci. U.S.A.* **1987**, *84*, 1769. (b) Baker, E. N.; Rumball, S. V.; Anderson, B. F. *Trends Biochem. Sci. (Pers. Ed.)* **1987**, *12*, 350.

0020-1669/89/1328-1414$01.50/0

Table I. Crystallographic Data for $[L_2Fe_2(\mu\text{-}O)(\mu\text{-}CO_3)_2]\cdot 4.25H_2O$

chem formula	$(C_9H_{21}N_3)_2Fe_2O(CO_3)_2(H_2O)_{4.25}$	λ, Å	Mo Kα (graphite monochromated)
fw	666.8	ρ_{calcd}, g cm^{-3}	1.42
space group	$P4/mnc$ (No. 128)	μ, cm^{-1}	8.99
T, °C	22	transmission coeff	0.87–1.00
a, Å	20.596 (7)	R^a	0.078
c, Å	16.404 (6)	$R_w{}^b$	0.056
V, Å^3	6958.48		
Z	8		

$^a R = \sum||F_o| - |F_c||/\sum|F_o|$. $^b R_w = [\sum_w(\Delta F)^2/\sum|F_o|^2]^{0.5}$.

tahedrally coordinated Fe^{III} centers are present, each of which binds a CO_3^{2-} (or HCO_3^-) ligand.

There are surprisingly few low-molecular-weight model complexes of iron(III) with coordinated carbonato ligands described in the literature. In fact, there appears to be only one crystallographically characterized complex. Hendrickson, Potenza, and Schugar[5] have recently described the tetranuclear complex $[Fe_4L'_2(\mu\text{-}O)_2(\mu\text{-}CO_3)_2]^{6-}$, where L′ represents the pentaanionic form of the ligand [(2-hydroxy-1,3-propanediyl)diimino]tetraacetic acid. This complex may be envisaged as a dimer of the dimeric (μ-oxo)(μ-carbonato)diiron(III) core. The carbonate is a bidentate bridging ligand. The complex spontaneously assembles in aqueous solution from a slurry of $Fe(OH)_3$, the ligand, and $NaHCO_3$.

Other attempts to model lactoferrin have been described, but no (carbonato)iron(III) complex has been obtained.[6]

Here we report our results on the hydrolysis reaction of $LFeCl_3$[7] in aqueous $NaHCO_3$, where L represents the cyclic triamine 1,4,7-trimethyl-1,4,7-triazacyclononane. At the outset of this work we hoped to generate the mononuclear complex $LFe(CO_3)Cl$ containing a bidentate carbonato ligand. Instead, we found that the binuclear complex $[L_2Fe_2(\mu\text{-}O)(\mu\text{-}CO_3)_2]$ formed—essentially quantitatively. Thus, as happens so often in aqueous ferric coordination chemistry, the thermodynamically stable (μ-oxo)diiron(III) core prevails over mononuclear alternatives.[8] We report the crystal structure, the magnetic properties, and the electronic spectrum of this binuclear complex.

Experimental Section

Preparation of $[L_2Fe_2O(CO_3)_2]\cdot 4.25H_2O$. To an aqueous solution (40 mL) of $NaHCO_3$ (2 g 23 mmol) was added $LFeCl_3$[7] (0.50 g 1.5 mmol). The suspension was gently heated to 60 °C for 30 min with stirring until a clear dark brown solution was obtained. The solvent was then removed under reduced pressure. The brown residue was treated with acetonitrile (20 mL); a colorless precipitate was filtered off and discarded. When the brown solution was allowed to stand in an open vessel for a few days, brown crystals of the title complex formed. Single crystals suitable for X-ray structure analysis were obtained in ca. 50% yield from acetonitrile solutions in an ultrasonic bath. Anal. Calcd for $[C_{20}H_{42}N_6O_7Fe_2]\cdot 4.25H_2O$: C, 36.02; H, 7.63; N, 12.60; Fe, 16.75. Found: C, 35.8; H, 7.6; N, 12.5; Fe, 16.3. IR (KBr): $\nu(CO_3)$ 1494 (vs), 1448 (vs), 1384 (vs) cm^{-1}. UV–vis (CH_3CN): 677 nm (ϵ = 145 L mol^{-1} cm^{-1}), 536 (270), 506 (690), 495 (sh), 445 (sh), 431 (1.3×10^3), 365 (sh), 340 (4.0×10^3), 243 (1.8×10^4), 990 (30).

Crystal Structure Determination. Intensities and lattice parameters of a brown cubic crystal of $[L_2Fe_2O(CO_3)_2]\cdot 4.25H_2O$ were measured on an AED II (Siemens) diffractometer. The lattice parameters (Table I) were obtained from a least-squares fit to the setting angles of 38 reflections with $7.5 < 2\theta < 30°$. An empirical absorption correction (ψ scans of five reflections with $6.4 < 2\theta < 36.5°$) was carried out. The structure was solved by standard Patterson and difference Fourier syntheses and refined[9] with anisotropic displacement parameters for all non-hydrogen atoms. Neutral-atom scattering factors and anomalous dispersion corrections for non-hydrogen atoms were taken from ref 10 and hydrogen atom scattering factors from ref 11. Since the space group cannot be uniquely determined from systematic absences, we have attempted the refinement in the possible alternative space groups. Smooth convergence of refinement cycles was only obtained in $P4/mnc$, yielding the smallest R value and reasonable bond distances and thermal parameters. Methylene and methyl hydrogen atoms were placed at calculated positions with d(C–H) at 0.96 Å and isotropic thermal parameters. The function minimized during refinement was $\sum w(|F_o| - |F_c|)^2$, where w =

Table II. Atom Coordinates (×10^4) and Temperature Factors (Å^2 × 10^3) for $[L_2Fe_2O(CO_3)_2]\cdot 4.25H_2O$

atom	x	y	z	$U_{eq}{}^a$
Fe(1)	5243 (1)	2283 (1)	0	22 (1)
Fe(2)	6535 (1)	1562 (1)	0	24 (1)
O(1)	5657 (3)	1500 (4)	0	29 (3)
O(2)	6658 (3)	2166 (3)	891 (4)	60 (3)
O(3)	5708 (3)	2694 (3)	−905 (4)	44 (2)
O(4)	6429 (3)	2856 (3)	−1885 (3)	38 (2)
C(0)	6272 (4)	2572 (4)	−1239 (5)	28 (3)
N(1)	4444 (3)	2016 (4)	855 (4)	47 (3)
N(2)	4612 (4)	3196 (4)	0	31 (4)
C(1)	4116 (6)	2622 (5)	−1125 (7)	118 (7)
C(2)	4221 (5)	3191 (5)	−734 (7)	87 (6)
C(3)	4011 (5)	1569 (6)	380 (6)	137 (7)
C(4)	4695 (5)	1624 (5)	1536 (5)	80 (5)
C(5)	5036 (6)	3785 (5)	0	48 (5)
N(3)	6704 (4)	731 (4)	−854 (4)	45 (3)
N(4)	7647 (4)	1485 (5)	0	35 (4)
C(11)	7377 (5)	773 (4)	−1159 (6)	66 (5)
C(12)	7827 (4)	1149 (6)	721 (6)	104 (6)
C(13)	6524 (7)	137 (5)	−409 (5)	134 (7)
C(14)	6249 (7)	766 (7)	−1541 (7)	163 (9)
C(15)	7926 (7)	2154 (7)	0	118 (10)
Wa(1)	8778 (3)	650 (3)	2528 (4)	51 (2)
Wa(2)	920 (4)	285 (4)	0	49 (3)
Wa(3)	9545 (3)	1460 (3)	1576 (4)	54 (2)
Wa(4)	2764 (3)	1117 (3)	1671 (4)	70 (3)
Wa(5)	2655 (2)	2345 (2)	2500	45 (2)
Wa(6)	0	0	3201 (8)	93 (5)

^{a} Equivalent isotropic U defined as one-third of the trace of the orthogonalized U_{ij} tensor.

Table III. Bond Lengths (Å) of the $[N_6Fe_2O(CO_3)_2]^{2+}$ Core

Fe(1)–Fe(2)	3.048 (2)		
Fe(1)–O(1)	1.826 (8)	Fe(1)–O(3)	1.959 (6)
Fe(1)–N(1)	2.232 (7)	Fe(1)–N(2)	2.285 (9)
Fe(2)–O(1)	1.813 (7)	Fe(2)–O(2)	1.937 (6)
Fe(2)–N(3)	2.238 (7)	Fe(2)–N(4)	2.297 (9)
O(2)–C(0a)	1.287 (10)	O(3)–C(0)	1.307 (9)
O(4)–C(0)	1.253 (10)	C(0)–O(2a)	1.287 (10)

Table IV. Bond Angles (deg) of the $[N_6Fe_2O(CO_3)_2]^{2+}$ Core

O(1)–Fe(1)–O(3)	98.8 (2)	O(1)–Fe(1)–N(1)	97.2 (3)
O(3)–Fe(1)–N(1)	160.7 (2)	O(1)–Fe(1)–N(2)	173.2 (3)
O(3)–Fe(1)–N(2)	85.6 (2)	N(1)–Fe(1)–N(2)	77.5 (3)
O(1)–Fe(1)–O(3a)	98.8 (2)	O(3)–Fe(1)–O(3a)	98.6 (3)
N(1)–Fe(1)–O(3a)	89.5 (2)	N(2)–Fe(1)–O(3a)	85.6 (2)
O(1)–Fe(1)–N(1a)	97.2 (3)	O(3)–Fe(1)–N(1a)	89.5 (2)
N(1)–Fe(1)–N(1a)	77.9 (3)	N(2)–Fe(1)–N(1a)	77.5 (3)
O(3a)–Fe(1)–N(1a)	160.7 (2)	O(1)–Fe(2)–O(2)	100.1 (2)
O(1)–Fe(2)–N(3)	95.9 (3)	O(2)–Fe(2)–N(3)	160.6 (3)
O(1)–Fe(2)–N(4)	172.0 (3)	O(2)–Fe(2)–N(4)	85.1 (2)
N(3)–Fe(2)–N(4)	78.0 (3)	O(1)–Fe(2)–O(2a)	100.1 (2)
O(2)–Fe(2)–O(2a)	98.0 (4)	N(3)–Fe(2)–O(2a)	89.9 (2)
N(4)–Fe(2)–O(2a)	85.1 (2)	O(1)–Fe(2)–N(3a)	95.8 (3)
O(2)–Fe(2)–N(3a)	89.9 (2)	N(3)–Fe(2)–N(3a)	77.5 (4)
N(4)–Fe(2)–N(3a)	78.0 (3)	O(2a)–Fe(2)–N(3a)	160.6 (3)
Fe(1)–O(1)–Fe(2)	113.8 (4)	Fe(2)–O(2)–C(0a)	132.1 (5)
Fe(1)–O(3)–C(0)	131.9 (5)	O(3)–C(0)–O(4)	119.6 (7)
O(3)–C(0)–O(2a)	119.2 (7)	O(4)–C(0)–O(2a)	121.2 (7)

(5) Jameson, D. L.; Xie, C.-L.; Hendrickson, D. N.; Potenza, J. A.; Schugar, H. J. *J. Am. Chem. Soc.* **1987**, *109*, 740.
(6) See for example: (a) Ainscough, E. W.; Brodie, A. M.; Plowman, J. E.; Brown, K. L.; Addison, A. W.; Gainsford, A. R. *Inorg. Chem.* **1980**, *19*, 3655. (b) Patch, M. G.; Simdo, K. P.; Carrano, C. J. *Inorg. Chem.* **1982**, *21*, 2972.
(7) Wieghardt, K.; Pohl, K.; Ventur, D. *Angew. Chem.* **1985**, *97*, 415; *Angew. Chem., Int. Ed. Engl.* **1985**, *24*, 392.
(8) Lippard, S. J. *Angew. Chem.* **1988**, *100*, 353; *Angew. Chem., Int. Ed. Engl.* **1988**, *27*, 344.
(9) All computations were carried out on an Eclipse computer using the SHELXTL program package.
(10) *International Tables for X-Ray Crystallography*; Kynoch: Birmingham, England, 1974; Vol. IV, pp 99, 149.
(11) Stewart, R. F.; Davidson, E. R.; Simpson, W. T. *J. Chem. Phys.* **1965**, *42*, 3175.

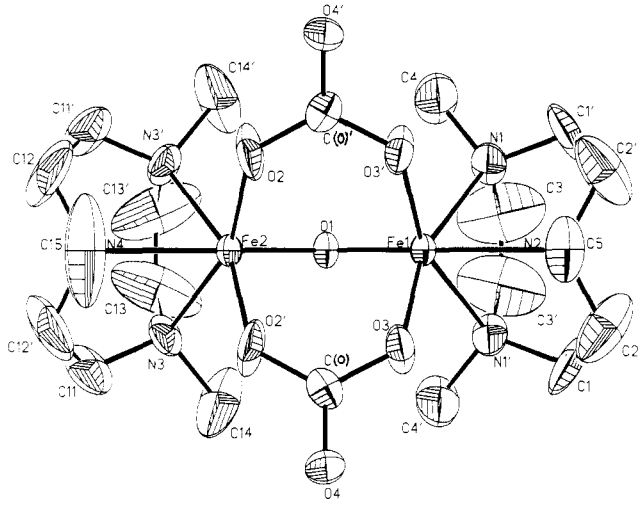

Figure 1. Structure of the molecule $(L_2Fe_2O(CO_3)_2]$.

$1/\sigma^2(F)$. Final atom coordinates are given in Tables III and IV, respectively.

Instrumentation and Physical Measurements. The magnetic susceptibility of a powdered sample of $[L_2Fe_2O(CO_3)_2]\cdot 4.25H_2O$ was measured by the Faraday method (Sartorius microbalance, Bruker research magnet, and Bruker automatic temperature control) in the temperature range 20–293 K. Diamagnetic corrections were applied in the usual manner with use of tabulated Pascal constants. UV–vis spectra were recorded on a Perkin-Elmer Lambda 9 spectrophotometer in the 250–1500-nm range.

Results and Discussion

The hydrolysis reaction of $LFeCl_3$ in an aqueous solution of sodium hydrogencarbonate at 60 °C yields a brown solution from which, after removal of the solvent water and extraction of the residue with acetonitrile, brown crystals of $[L_2Fe_2O(CO_3)_2]\cdot 4.25H_2O$ were obtained. Recrystallization of this material from acetonitrile in an ultrasonic bath yielded crystals of X-ray quality.

The molecular structure of the neutral molecule is shown in Figure 1. It is a binuclear complex containing a (μ-oxo)bis(μ-carbonato)diiron(III) core with a tridentate cyclic amine capping each iron(III) center. Two CO_3^{2-} anions function as bidentate bridging ligands as in Schugar's compound.[5]

The binuclear species has crystallographically required *m* site symmetry, which is not compatible with the ($\lambda\lambda\lambda$) or ($\delta\delta\delta$) conformation of the five-membered chelate rings of the facially coordinated tridentate cyclic amine. Thus, it is statistically disordered in the tetragonal space group. This is manifested by large anisotropic thermal parameters for the methylene carbon atoms C(1), C(2), C(3), C(11), C(12), and C(13) (Table S3, supplementary material). This is quite common for dimeric complexes containing coordinated 1,4,7-triazacyclononane ligands.[12b]

The bent Fe–O–Fe unit (113.8 (4)°) contains the shortest Fe–O bonds (average 1.820 Å) in the structure. They are among the longest reported for oxo-bridged binuclear units. In the corresponding complex $[L_2Fe_2(\mu\text{-}O)(\mu\text{-}CH_3CO_2)_2](ClO_4)_2\cdot H_2O$[12] the Fe–O–Fe bond angle is 119.7 (1)° and the $Fe-O_{oxo}$ bond lengths are shorter (average 1.800 Å). Interestingly, the Fe–N bonds trans to the oxo bridge are longer than those in cis positions ($(Fe-N_{trans}) - (Fe-N_{cis}) = 0.056$ Å); in the bis(μ-acetato) analogue this difference is 0.070 Å. The Fe–O bonds of the carbonato bridges are shorter than the corresponding bonds of μ-acetato bridges ($(Fe-O_{carbonate}) - (Fe-O_{acetate}) = -0.086$ Å). Thus, the carbonato groups are more tightly bound to the iron(III) centers than the acetato ligands in the respective complexes.

Interestingly, the chemistry also supports this view. HCO_3^- is a stronger nucleophile than the $CH_3CO_2^-$ ion. HCO_3^- replaces the acetato bridges of $[L_2Fe_2(\mu\text{-}O)(\mu\text{-}CH_3CO_2)]^{2+}$ in aqueous solution; the μ-carbonato complex forms readily.

Table V. Hydrogen-Bonded Contacts in $[L_2Fe_2(\mu\text{-}O)(\mu\text{-}CO_3)_2]\cdot 4.25H_2O$ (O–H···O < 3.0 Å)

O(4)–Wa(5)	2.750 (8)	Wa(1)–Wa(3)	2.777 (9)
O(4)–Wa(1)	2.668 (7)	Wa(2)–Wa(2′)	2.805 (11)
Wa(2)–Wa(3)	2.835 (10)	Wa(3)–Wa(1′)	2.804 (12)
Wa(4)–Wa(5)	2.882 (8)		

Each of the terminal oxygen atoms of the μ-carbonato bridges (O(4)) forms two strong hydrogen bonds to two water molecules (Wa(1) and Wa(5); see Table V). In addition, a number of hydrogen bonds between the water molecules of crystallization are present; the O···O distances range from 2.67 to 2.88 Å.

Magnetic susceptibility measurements were carried out on a solid sample of $[L_2Fe_2O(CO_3)_2]\cdot 4.25H_2O$ by using a Faraday method in the temperature range 20–293 K. The temperature-dependent magnetic behavior was modeled by using the theory of Heisenberg, Dirac, and Van Vleck for magnetic coupling in a binuclear system. Neither spin–orbit coupling nor zero-field splitting was modeled. The expression for the temperature-dependent susceptibility may be derived from the general isotropic exchange Hamiltonian, $H = -2JS_1\cdot S_2$, where $S_1 = S_2 = {}^5/_2$. A Curie-type term was required to correct for 0.04% of a paramagnetic, monomeric impurity ($S = {}^5/_2$). The least-squares fit for $[L_2Fe_2O(CO_3)_2]\cdot 4.25H_2O$ gave $g = 1.999$ and $J = -91$ (1) cm^{-1}.[17] This value is in the range −80 to −105 cm^{-1} usually observed for simple (μ-oxo)diiron(III) compounds,[13] but it is significantly smaller than those values found for complexes containing the (μ-oxo)bis(μ-carboxylato)diiron(III) core[8,12] (∼−120 or −134 cm^{-1} measured for methemerythrin from *Phascolopis* (*syn Golfingia*) *gouldii*).[14] Interestingly, for Schugar's μ-oxo–μ-carbonato-bridged species an intradimer antiferromagnetic coupling of −63.4 cm^{-1} has been reported.[5] This is surprising since it is currently accepted that short $Fe-O_{oxo}$ bonds in the Fe–O–Fe unit lead to strong intradimer coupling.[5] In the present case the $Fe-O_{oxo}$ bond lengths are identical with those observed in Schugar's tetramer. On the other hand, in all complexes of the (μ-oxo)bis(μ-carboxylato)diiron(III) type the $Fe-O_{oxo}$ bonds are significantly shorter and in all instances stronger antiferromagnetic intradimer exchange coupling has been observed.

In Lippard's complex $[\{HB(pz)_3\}_2Fe_2(\mu\text{-}O)(\mu\text{-}PO_4Ph_2)_2]$ the dimensions of the (μ-oxo)bis(μ-diphenyl phosphato)diiron(III) core are $Fe-O_{oxo}$ = 1.812 (5), 1.804 (5) Å and Fe–O–Fe = 134.7°; an antiferromagnetic superexchange coupling constant of $J = -98$ cm^{-1} has been reported.[15] This is of the same magnitude as is observed here for $[L_2Fe_2O(CO_3)_2]\cdot 4.25H_2O$.

A deeper understanding of these superexchange phenomena obviously requires a detailed analysis of the actual magnetic orbitals and their relative overlap. It is noted in this respect that the μ-oxo-bridged diiron(III) complexes with two additional carbonato, phosphato, or carboxylato bridging groups may to a first approximation be viewed as face-sharing bioctahedral, whereas in Schugar's complex the Fe–O–Fe unit is bridged by only *one* additional carbonato group, which leads to an edge-sharing bioctahedral situation. It is conceivable that superexchange pathways occur that are mediated by different orbital interactions in complexes with differently bridged diiron(III) cores. The currently accepted model taking into account only $Fe-O_{oxo}$ distances (and Fe–O–Fe angles)[18] may be an oversimplification.

(12) (a) Chaudhuri, P.; Wieghardt, K.; Nuber, B.; Weiss, J. *Angew. Chem.* **1985**, *97*, 774; *Angew. Chem. Int. Engl.* **1985**, *24*, 778. (b) Hartman, J. R.; Rardin, R. L.; Chaudhuri, P.; Pohl, K.; Wieghardt, K.; Nuber, B.; Weiss, J.; Papaefthymiou, G. C.; Frankel, R. B.; Lippard, S. J. *J. Am. Chem. Soc.* **1987**, *109*, 7387.

(13) (a) Thich, J. A.; Toby, B. H.; Powers, D. A.; Potenza, J. A.; Schugar, H. J. *Inorg. Chem.* **1981**, *20*, 3314. (b) Murray, K. S. *Coord. Chem. Rev.* **1974**, *12*, 1.

(14) Dawson, J. W.; Gray, H. B.; Hoenig, H. E.; Rossman, G. R.; Schredder, J. M.; Wang, R. H. *Biochemistry* **1972**, *11*, 461.

(15) Armstrong, W. H.; Lippard, S. J. *J. Am. Chem. Soc.* **1985**, *107*, 3730.

(16) Schugar, H. J.; Rossman, G. R.; Barraclough, C. G.; Gray, H. B. *J. Am Chem. Soc.* **1972**, *94*, 2683.

(17) We thank Dipl.-Ing. P. A. Fleischhauer and Prof. W. Haase (TH Darmstadt) for the susceptibility measurements.

(18) (a) Mukherjee, R. N.; Stack, T. D. P.; Holm, R. H. *J. Am. Chem. Soc.* **1988**, *110*, 1850. (b) Alder, J.; Ensling, J.; Gütlich, P.; Bominaar, E. L.; Guillin, J.; Trautwein, A. X. *Hyperfine Interact* **1988**, *42*, 869.

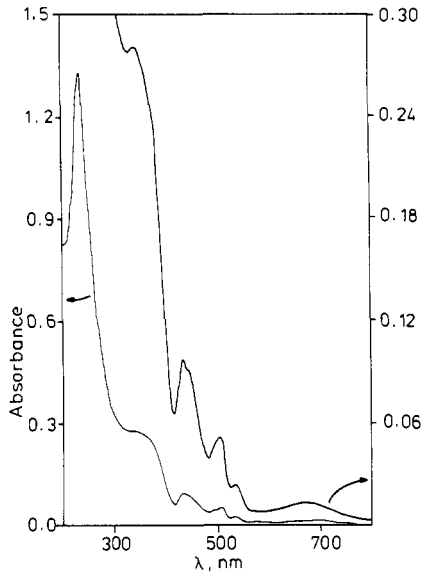

Figure 2. Electronic spectrum of $[L_2Fe_2O(CO_3)_2]\cdot 4.25H_2O$ in acetonitrile ([dimer] = 0.83×10^{-4} M, 1-cm cell).

Figure 2 shows the solution electronic spectrum of $[L_2Fe_2O(CO_3)_2]\cdot 4.25H_2O$ in acetonitrile. Three moderately intense absorption bands in the visible region (990, 677, 536 nm) may be assigned to ligand field transitions of six-coordinate $^6A_1$ ferric ions.[16] The binuclear species then exhibits five intense absorption bands at 506, 445 (sh), 431, 365 (sh), and 340 nm with molar absorption coefficients exceeding 10^3 L mol^{-1} cm^{-1} (except the band at 506 nm), which may be assigned to simultaneous-pair excitation electronic bands and/or Fe–O–Fe charge-transfer bands by following Gray's analysis of the electronic spectrum of $Na_4[(FeEDTA)_2O]\cdot 12H_2O$.[16] The spectrum of $[L_2Fe_2O(CO_3)_2]$ is quite similar to that reported for $[L_2Fe_2O(CH_3CO_2)_2](ClO_4)_2\cdot H_2O$.[12]

Acknowledgment. We thank the Fonds der Chemischen Industrie for financial support of this work.

Supplementary Material Available: A full table of crystallographic data (Table S1) and tables containing calculated positional parameters of hydrogen atoms (Table S2), anisotropic thermal parameters of nonhydrogen atoms (Table S3), and intraligand bond distances (Table S4) and angles (Table S5) (5 pages); a table of observed and calculated structure factor amplitudes (Table S6) (12 pages). Ordering information is given on any current masthead page.

Contribution from the Department of Chemistry, University of Texas at Austin, Austin, Texas 78712

Synthesis and Characterization of a New Potentially Ditopic Receptor, 1,4,7,10-Tetraoxa-13,16,19,22-tetraazacyclotetracosane, and the X-ray Crystal Structure of Its Mononuclear Copper(II) Complex

Jonathan L. Sessler,* John W. Sibert, Jeffrey D. Hugdahl, and Vincent Lynch

Received September 29, 1988

In recent years there has been considerable interest in the development of new macrocyclic binucleating ligands.[1-5] Of particular interest are ditopic receptors containing both hard and soft sites, as these could have a variety of applications in extending the range and scope of coordination chemistry.[6,7] They could, for instance, act to stabilize homodimeric transition-metal complexes in which the two metal centers are in two different oxidation states or perhaps support the formation of heterodimeric metal complexes in which two very different cations (e.g. from group I and the first transition series) are bound within the same macrocyclic framework. In addition, they could act as models for naturally occurring metalloprotein systems.[8-10] Although a number of novel ditopic receptors have now been reported, few of these have relied on using polyaza subunits as one or more of the binding components.[5,11] We therefore sought to develop a crown ether system that would contain, *within the same macrocyclic ligand*, both polyoxa and polyaza subunits as potentially hard and soft binding sites, respectively; we report here the synthesis and characterization of 1,4,7,10-tetraoxa-13,16,19,22-tetraazacyclotetracosane (**2**) and the structure of its 1:1 Cu^{2+} complex **3**.

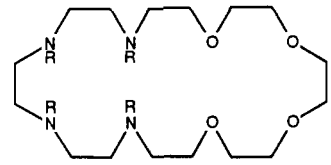

1 R = Ts

2 R = H

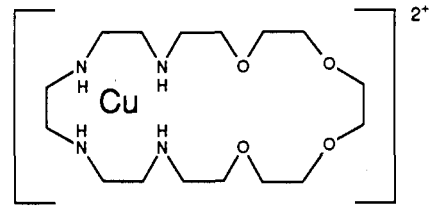

3

Experimental Section

NMR spectra were obtained in $CDCl_3$ with Me_4Si as an internal standard and recorded on a General Electric QE-300 spectrometer. Routine electron impact (EI) mass spectra were measured with a Finnigan MAT 4023 or a Bell and Howell 21-110B instrument. Low-resolution fast atom bombardment mass spectrometry (FAB MS) was performed by using a Finnigan MAT TSQ-70 instrument using 3-nitrobenzyl alcohol as the matrix. Electronic spectra were recorded in methanol on a Beckman DU-7 spectrophotometer. Pentaethylene glycol di-*p*-toluenesulfonate (95% pure) was purchased from Aldrich Chemical Co.

Preparation of 13,16,19,22-Tetratosyl-1,4,7,10-tetraoxa-13,16,19,22-tetraazacyclotetracosane (1). 1,4,7,10-Tetratosyl-1,4,7,10-tetraazadecane[12] (4.74 g, 6.2 mmol) was added to a stirred suspension of 0.35 g of NaH (13 mmol) in 150 mL of DMF. The reaction mixture was stirred and heated at 100 °C under N_2. After 1 h, pentaethylene glycol di-*p*-toluenesulfonate (3.40 g, 6.22 mmol), dissolved in 100 mL of DMF, was added dropwise. The temperature was kept at 100 °C for 20 h. Evap-

(1) Lehn, J. M. *Pure Appl. Chem.* **1980**, *52*, 2441–2459.
(2) Pilkington, N. H.; Robson, R. *Aust. J. Chem.* **1970**, *23*, 2225–2236.
(3) Hoskins, B. F.; McLeod, N. J.; Schaap, H. A. *Aust. J. Chem.* **1976**, *29*, 515–521.
(4) Groh, S. E. *Isr. J. Chem.* **1976/77**, *15*, 277–307.
(5) Bencini, A.; Bianchi, A.; Garcia-Espana, E.; Giusti, M.; Mangani, S.; Micheloni, M.; Orioli, P.; Paoletti, P. *Inorg. Chem.* **1987**, *26*, 1243–1247.
(6) van Staveren, C. J.; van Eerden, J.; van Veggel, F. C. J. M.; Harkema, S.; Reinhoudt, D. N. *J. Am. Chem. Soc.* **1988**, *110*, 4994–5008.
(7) Carroy, A.; Lehn, J.-M. *J. Chem. Soc., Chem. Commun.* **1986**, 1232–1234.
(8) Coughlin, P. K.; Dewan, J. C.; Lippard, S. J.; Watanabe, E.; Lehn, J. M. *J. Am. Chem. Soc.* **1979**, *101*, 265–266.
(9) Coughlin, P. K.; Lippard, S. J. *J. Am. Chem. Soc.* **1981**, *103*, 3228–3229.
(10) Sorrell, T. N.; Jameson, D. L.; O'Connor, C. J. *Inorg. Chem.* **1984**, *23*, 190–195.
(11) Bencini, A.; Bianchi, A.; Garcia-Espana, E.; Mangani, S.; Micheloni, M.; Orioli, P.; Paoletti, P. *Inorg. Chem.* **1988**, *27*, 1104–1107.
(12) Bencini, A.; Fabbrizzi, L.; Poggi, A. *Inorg. Chem.* **1981**, *20*, 2544–2549.

0020-1669/89/1328-1417$01.50/0